

LIBRARY USE ONLY

5146  
TM95-2143

NUWC-NPT Technical Memorandum 952143

Copy 1

Naval Undersea Warfare Center Division  
Newport, Rhode Island



**ELECTROMAGNETIC FORCE CALCULATION FOR  
A TORPEDO FUEL SHUTOFF SOLENOID VALVE**

C. P. Cho  
Weapon Technology and Undersea Systems Department

R. J. Angeli  
Torpedo Systems Department

G. P. Davies  
Vitro Corporation

30 November 1995

**UNCLASSIFIED**  
NAVAL UNDERSEA WARFARE CENTER  
DIVISION NEWPORT  
NEWPORT, RHODE ISLAND 02841-1708  
RETURN TO: TECHNICAL LIBRARY

Approved for public release; distribution is unlimited.

LIBRARY USE ONLY

Report Documentation Page			Form Approved OMB No. 0704-0188		
Public reporting burden for the collection of information is estimated to average 1 hour per response, including the time for reviewing instructions, searching existing data sources, gathering and maintaining the data needed, and completing and reviewing the collection of information. Send comments regarding this burden estimate or any other aspect of this collection of information, including suggestions for reducing this burden, to Washington Headquarters Services, Directorate for Information Operations and Reports, 1215 Jefferson Davis Highway, Suite 1204, Arlington VA 22202-4302. Respondents should be aware that notwithstanding any other provision of law, no person shall be subject to a penalty for failing to comply with a collection of information if it does not display a currently valid OMB control number.					
1. REPORT DATE <b>30 NOV 1995</b>		2. REPORT TYPE <b>Technical Memo</b>		3. DATES COVERED <b>30-11-1995 to 30-11-1995</b>	
4. TITLE AND SUBTITLE <b>Electromagnetic Force Calculation for a Torpedo Fuel Shutoff Solenoid Valve</b>				5a. CONTRACT NUMBER	
				5b. GRANT NUMBER	
				5c. PROGRAM ELEMENT NUMBER	
6. AUTHOR(S) <b>C. Cho; R. Angeli; G. Davies</b>				5d. PROJECT NUMBER	
				5e. TASK NUMBER	
				5f. WORK UNIT NUMBER	
7. PERFORMING ORGANIZATION NAME(S) AND ADDRESS(ES) <b>Naval Undersea Warfare Center Division,1176 Howell Street,Newport,RI,02841</b>				8. PERFORMING ORGANIZATION REPORT NUMBER <b>TM 952143</b>	
9. SPONSORING/MONITORING AGENCY NAME(S) AND ADDRESS(ES)				10. SPONSOR/MONITOR'S ACRONYM(S)	
				11. SPONSOR/MONITOR'S REPORT NUMBER(S)	
12. DISTRIBUTION/AVAILABILITY STATEMENT <b>Approved for public release; distribution unlimited</b>					
13. SUPPLEMENTARY NOTES <b>NUWC2015</b>					
14. ABSTRACT <b>The electromagnetic forces induced in a fuel shutoff solenoid valve have been analyzed using finite element analysis (FEA) models and lumped magnetic circuit equations. The purpose of this study was to investigate the electromagnetic force capability of the current solenoid valve design and to aid in finding future design refinements for improved reliability with minimal changes. The calculated magnetic force results are compared with experimental measurements made from the design of record fuel shutoff valves, and good correlation is shown to exist. The developed FEA models and lumped magnetic circuit equations can be used in future solenoid valve development and optimization.</b>					
15. SUBJECT TERMS <b>solenoid valve</b>					
16. SECURITY CLASSIFICATION OF:			17. LIMITATION OF ABSTRACT <b>Same as Report (SAR)</b>	18. NUMBER OF PAGES <b>26</b>	19a. NAME OF RESPONSIBLE PERSON
a. REPORT <b>unclassified</b>	b. ABSTRACT <b>unclassified</b>	c. THIS PAGE <b>unclassified</b>			

## **ABSTRACT**

The electromagnetic forces induced in a fuel shutoff solenoid valve have been analyzed using finite element analysis (FEA) models and lumped magnetic circuit equations. The purpose of this study was to investigate the electromagnetic force capability of the current solenoid valve design and to aid in finding future design refinements for improved reliability with minimal changes. The calculated magnetic force results are compared with experimental measurements made from the design of record fuel shutoff valves, and good correlation is shown to exist. The developed FEA models and lumped magnetic circuit equations can be used in future solenoid valve development and optimization.

## **ADMINISTRATIVE INFORMATION**

This memorandum was prepared under Code 82 internal funding.

C. P. Cho and R. J. Angeli are located at the Naval Undersea Warfare Center Division, Newport, RI 02841-1708 and G. P. Davies is located at Vitro Corporation in Middletown, RI 02842.

## **ACKNOWLEDGMENT**

The authors gratefully acknowledge the assistance of Dr. S. Reddy of Oregon State University in evaluating the mathematical equations. Thanks also go to M. C. Rodamaker of MCR Associates, Inc., Sunnyvale, CA for ANSYS modeling and the many suggestions provided.

## INTRODUCTION

This memorandum presents an electromagnetic force analysis of a torpedo fuel shutoff solenoid valve (FSSV) using finite element analysis (FEA) models and lumped magnetic circuit equations. The primary objectives were to investigate the electromagnetic force generation capability of the current design and to provide recommendations for future performance and reliability improvements. Experimental data were measured by the Naval Systems Division at Westinghouse and at the Naval Undersea Warfare Center (NUWC) Division, Newport, RI, Newport Power Electronics Laboratory, and Composite Material Laboratory.

### Background

Due to the recent technological advancement made in the area of control electronics there is an increasing use of electronically controlled solenoids and actuators in many different applications. Some of these electromechanical devices are replacing existing vacuum operated solenoids and actuators to achieve a faster response and a more precise positioning, while others are added to perform new functions. Also, in the area of the automobiles fuel injection, future injector solenoids are required to provide a much faster response than today's. This is leading to solenoids having new configurations and using new materials. Optimization of these solenoids often requires 3-dimensional magnetic field analysis. Developing tools to conduct such analysis, while taking into account the extremely important effects of eddy currents and moving parts is an essential element of research in the area of fast acting solenoids.

The FSSV operates as an electromagnetic solenoid, as shown in figures 1 and 2. A solenoid consists of plunger, coil winding, and a pole piece. The winding is energized with a dc voltage; the plunger in this case is the armature, which moves to open the valve, thereby allowing fuel flow when current passes through the winding; and the stop is the pole piece. When the dc voltage is removed, the armature moves to close the valve via a spring. The valve is sealed with an O-ring. References 1 and 2 contain further details on electromagnetic solenoids.

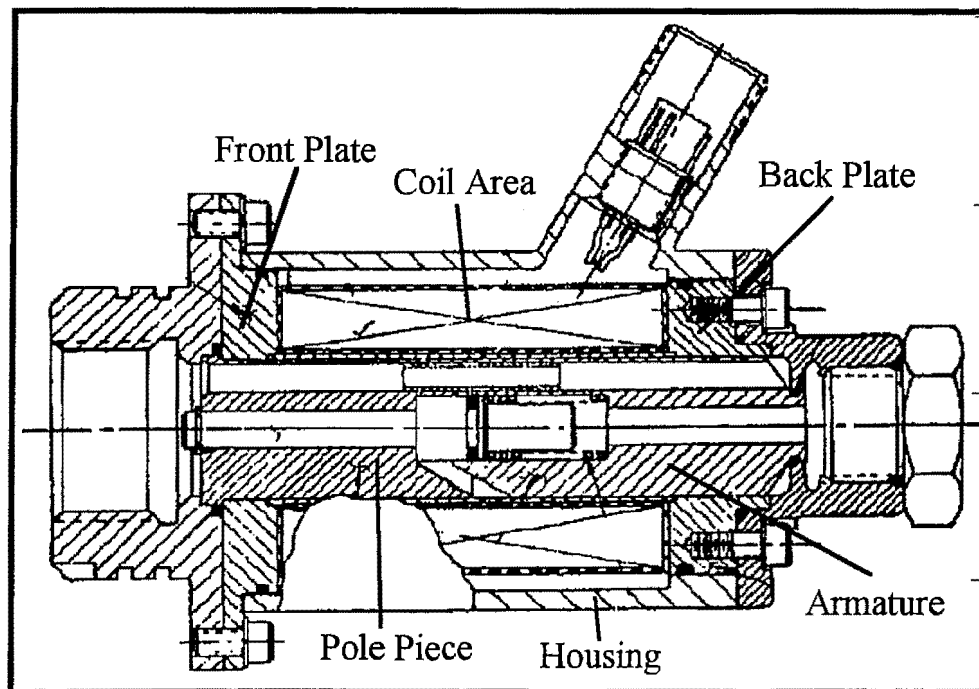


*Figure 1. Fuel Shutoff Solenoid Valve Drawing*

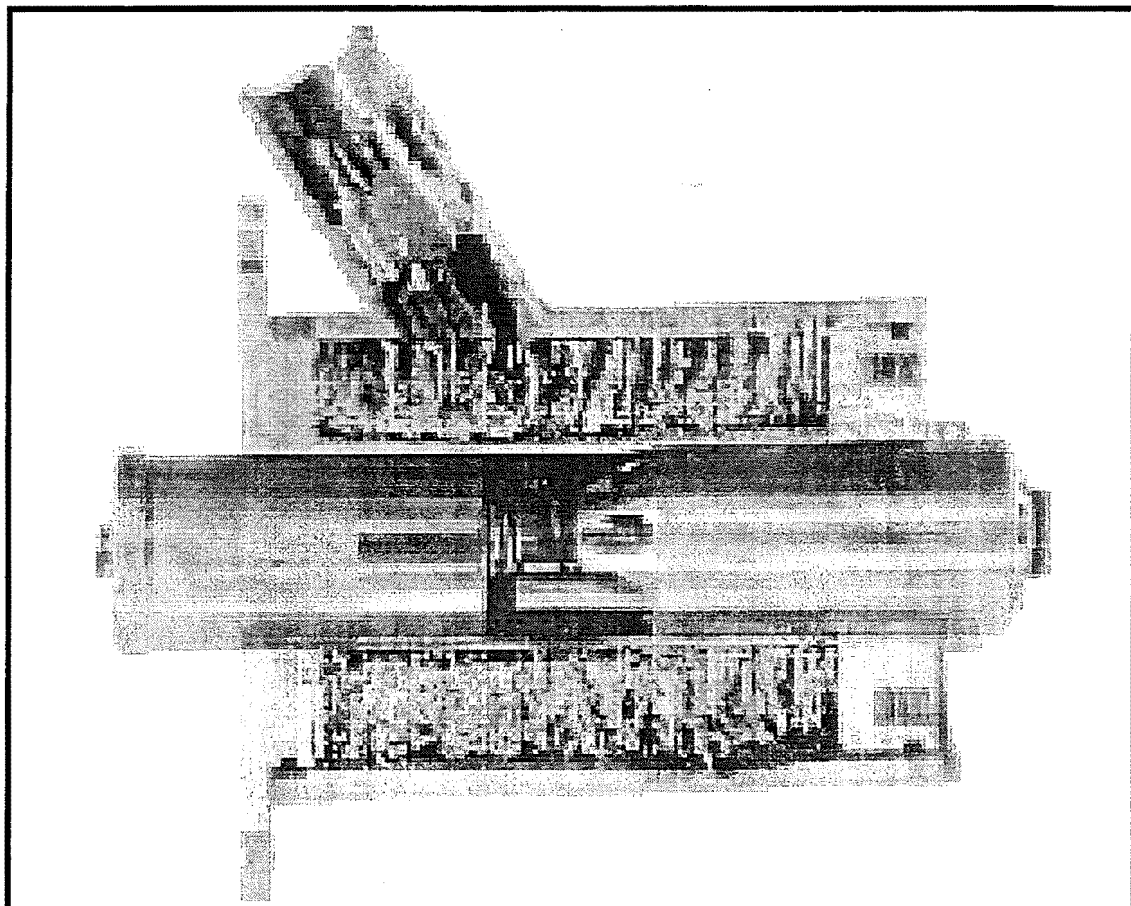


*Figure 2. Cutaway Picture of Solenoid*

## **Fuel Solenoid Shutoff Valve Description**

The FSSV is a device used to allow or prevent the pumping of fuel from the fuel tank to the torpedo engine. The FSSV is also used during the fuel tank filling operation and as a detonation trap for the tank. The seven holes in both the armature (plunger) and pole piece (stop) are used as fuel transport channels and were sized to break up a potential pressure wave in the event of a detonation downstream from the valve. The armature, pole piece, and coil housing are presently fabricated from 416 stainless steel (416 SS). Corrosion-resistant materials are required in the flow path (armature and pole piece) because of the potential sea-water contamination, and it is required for the housing material because of the environment in which it is located.

The FSSV is a normally closed valve that uses a spring to prevent armature motion. An O-ring bore seal is used at the forward end of the valve to prevent leakage past the closed valve. The piston (guide) seals the center hole of the armature from fuel downstream of the valve with an O-ring/glyd ring arrangement. The FSSV is presently energized with 25-27 dc voltage in a ramped function. As the armature moves over the piston toward the pole piece, fuel is allowed to flow from the tank to the fuel pump.

## **Method of Analysis**

To predict the solenoid electromagnetic forces and to perform a tradeoff study (armature geometry, applied current, and coil-winding turns), it is necessary to accurately calculate the magnetic field throughout the solenoid structure. There are many kinds of field calculation methods, and each method has a different level of accuracy.

FEA 2-D nonlinear models were used to analyze the solenoid considered in this study. Using FEA models permits the inclusion of intricate physical shapes of the solenoid and nonlinear magnetic material properties for an accurate analysis. The main disadvantage of using the FEA method is the excessive engineering effort and computer resources required to set up the FEA model and to analyze the results. To reduce such problems, mesh generation, solution process, and result calculations of the FEA modeling and analysis have been parameterized using two macro programs. These programs alleviate the need to create a new mesh for each geometric, material, or armature position change (reference 3).

The primary objectives of the FEA method used in this study were to investigate the flux paths in the solenoid, to check the maximum flux density in the structure for saturation, and to evaluate electromagnetic forces and inductance values. The FEA-calculated flux paths were used in developing the lumped parameter magnetic circuit models of the solenoid; these models can be used as a part of a design tool for future solenoid valves.

All the FEA in this study used a quasi-static, nonlinear magnetic-field analysis. A quasi-static magnetic field is a dynamic field in which the effect of the eddy currents and inertia are neglected. For example, the magnetic field produced by changes in armature position can be assumed to be a series of magneto-static fields, which are quasi-static magnetic fields. This assumption is based on the premise that the magnetic fields produced by the winding-current sources are not affected by the other dynamic effects, such as eddy currents, magnetic hysteresis, and the rise and fall time of

the applied current (reference 4). A series of quasi-static, nonlinear magnetic analyses was performed in this study to determine the electromagnetic forces. Inductance values were also calculated using an FEA model.

The lumped parameter magnetic circuit equation was used in this study because it relates the solenoid geometric and material characteristics to the solenoid output forces through closed-form algebraic expressions. The impact of geometry, excitation, and material property changes on the overall system can be assessed, and new designs may be rapidly and accurately considered without going through time-consuming FEA modeling and the construction of costly prototypes.

Lumped parameter magnetic equation development is not as simple as modeling electrical circuits. In electrical circuits, electric current remains principally in the intended conductive paths, and there is very little leakage. In magnetic circuits, however, magnetic flux is not principally confined to magnetic material, and there is a significant amount of flux leakage. Accordingly, flux leakage paths for the magnetic flux must be included to develop more accurate lumped parameter magnetic circuit models. Consequently, in this study, FEA models and resulting flux distribution plots were used to identify leakage flux paths so that accurate lumped parameter magnetic circuit models can be developed.

## **FINITE ELEMENT ANALYSIS**

Solenoid electromagnetic forces were analyzed using FEA models that find the magnetic vector potential  $A$  and magnetic flux density  $B$  throughout the 2-D region containing nonlinear magnetic materials (equations 5 and 6). The FEA model requires that the region be divided into a number of finite elements having vertices called grids (nodes). The location of the grids, material property (permeability), boundary conditions, and excitation (current density) of each element are required as input data. In addition to calculating  $A$  and  $B$  throughout the region and plotting the flux pattern, the program computes the flux linkage  $\lambda$ , magnetic energy, and magnetic co-energy,  $W_M$  and  $W_{co}$ , respectively, in the region of interest.

These FEA-calculated electromagnetic forces were compared with lumped parameter magnetic circuit calculations and experimental measurements to verify the accuracy of the FEA models, to optimize performance, and to minimize future solenoid valve development cost.

### **FEA Model Description**

It can be seen from figures 1 and 2 that the solenoid is symmetric about its axis, thus allowing it to be modeled by a one-half section of the full solenoid. The magnetic force calculated by this symmetric model is the force generated over 360°. Because the FEA package is limited in the total number of possible grids, modeling a one-half section using axial symmetry permits a finer finite element mesh. The outline of the 2-D FEA mesh used for the solenoid model with meshes and flux distribution is illustrated in figure 3.

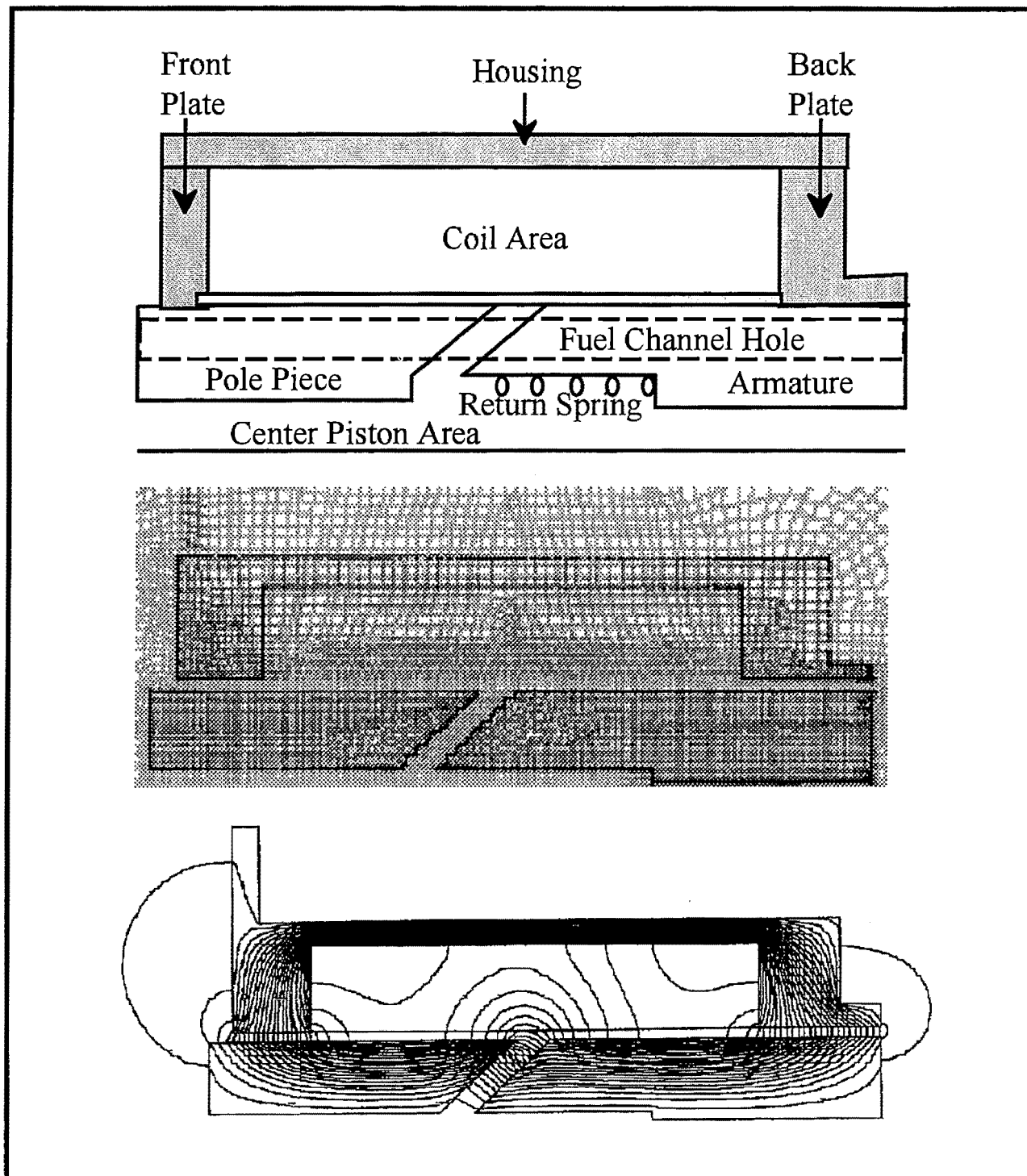


*Figure 3. Axi-Symmetric FEA Model*



In the 2-D FEA model, the higher-order quad element-type and triangular element-type were used. Figure 4 shows a cross-sectional view of the armature and pole piece. There are seven fuel channel holes and a center piston hole. A side view of the pole piece and armature with fuel channel holes (dotted lines) is depicted in figure 5. In the 2-D axi-symmetric FEA model, the fuel channel holes were subtracted from the armature and pole piece to determine the effective plunger radius.

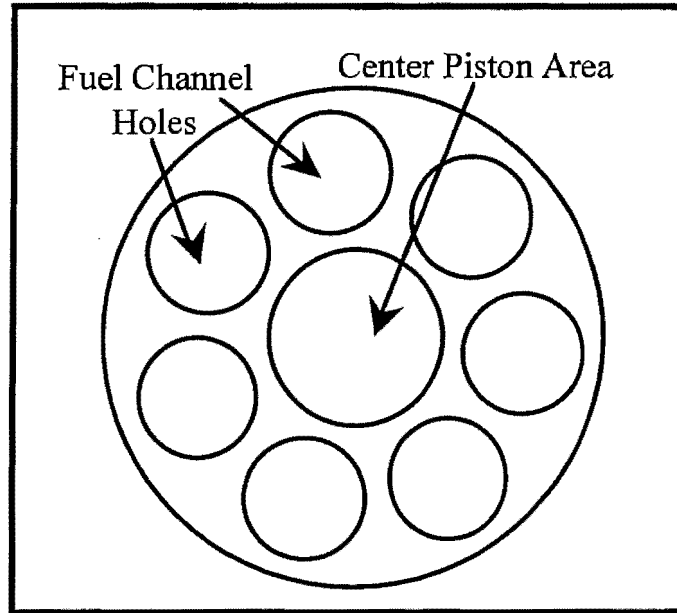


*Figure 4. Fuel Channel Holes in Armature*

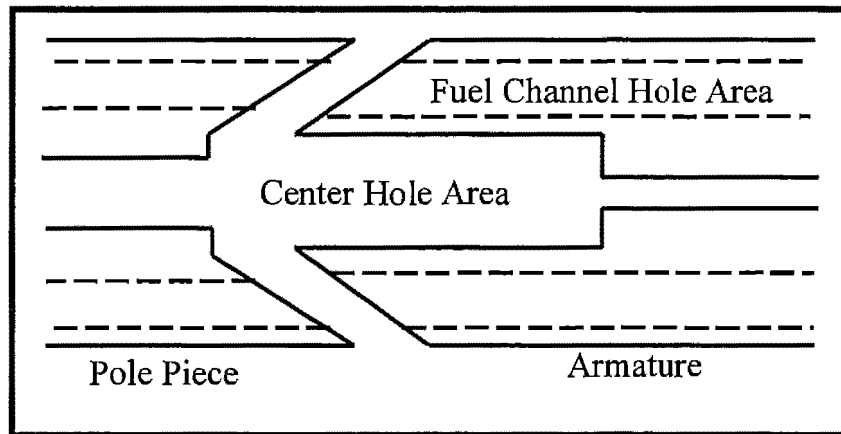


*Figure 5. Side View of Pole Piece and Armature*

The effective fuel channel area, as shown in figure 6, was calculated by totaling the seven fuel-channel areas. This effective fuel-channel area was then subtracted from the total armature and pole-piece axial cross-sectional area. Winding current density was calculated by dividing current in the coil by the total winding area.

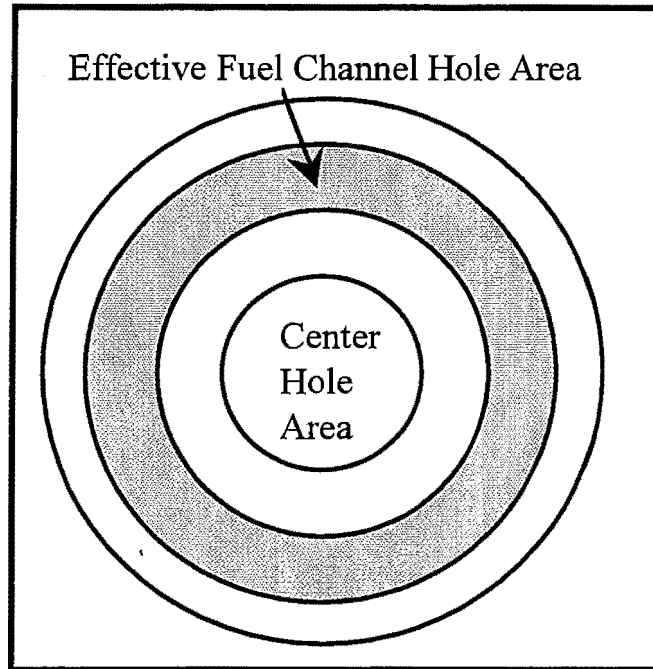


*Figure 6. Effective Fuel Channel Hole Area*

Two different FEA models (see figures 7 and 8) were compared to determine the accuracy of the calculations. In model A, the effective fuel-channel areas were subtracted from the center hole and piston area (see figure 7), and in the model B, the effective fuel-channel areas were subtracted from their actual locations in the pole piece and armature (see figure 8). The magnetic forces for the two models were calculated at the same excitation. If the differences were small, the magnetic force was primarily affected by the total amount of magnetic material in the flux path, not the location. The magnetic forces were compared, and no significant difference was found as shown in table 1. Model A was used throughout this study because of its ease of change and calculation.

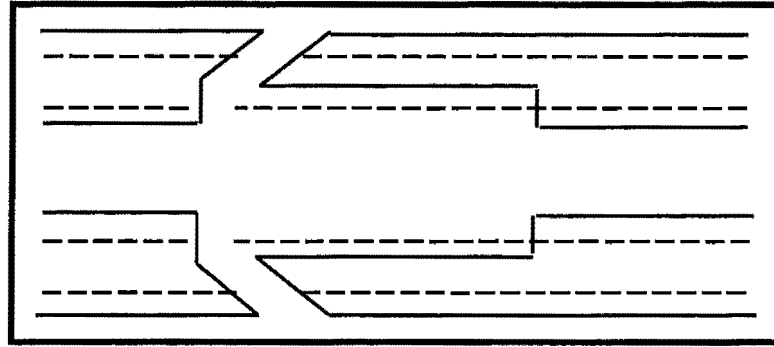


*Figure 7. Model A*

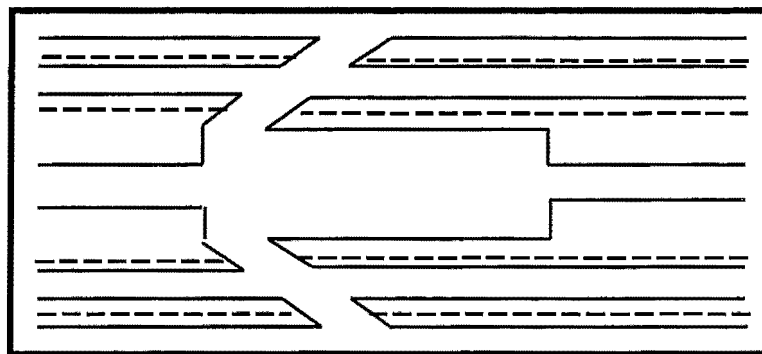


*Figure 8. Model B*

*Table 1. Model A and B Comparison (430 SS)*

Force	Model A	Model B	Difference
Air Gap 5.5 mm	51.3 N	49.4 N	4 %
Current 1.25 A			

### **FEA Model Checking**

The accuracy of the FEA field-calculation results depends primarily on the resolution or density of meshing and the element type used. This section reports how the 2-D FEA models were checked for force convergence to verify the accuracy of the model results (reference 4).

Figure 9 shows the total magnetic force on the armature versus total the number of elements in the FEA models. For the total number of elements above 1700, the resulting accuracy does not improve, but the computer operating time (CPU time) goes up as a square function of the total number of elements.

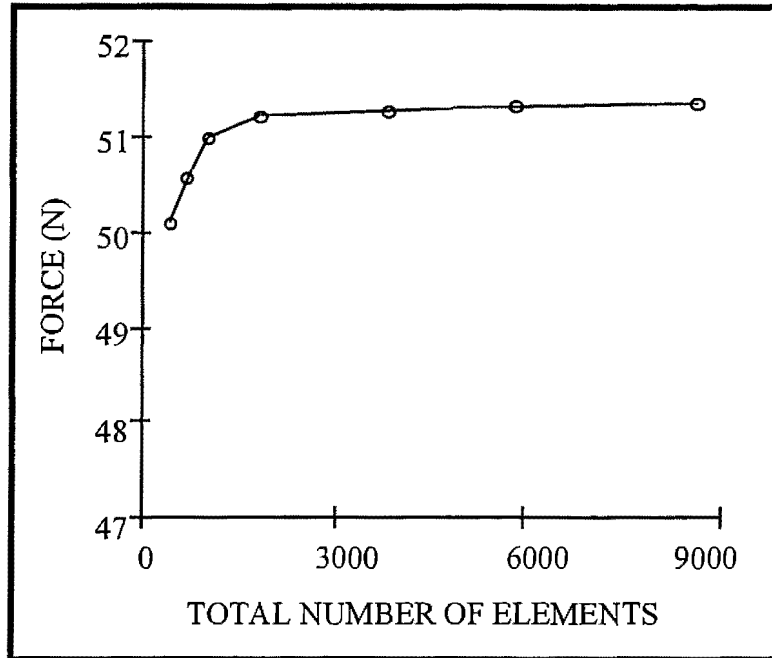


*Figure 9. Mesh Density vs Force*

The total number of elements for optimum results is 1766 for the given solenoid geometry. Any particular FEA model has its own optimum number of elements that depend on geometry and type of excitation; therefore, an FEA model convergence test is a necessary step before processing a number of FEA models. The time spent to check the accuracy of the model in the beginning of the process produces more accurate final results.

The accuracy of the FEA-calculated force results was compared with measured force data (see figure 10). Since the FEA model does not include all the mechanical friction, O-ring sticking force, inertia, and eddy current effects, the difference in this comparison is reasonable.

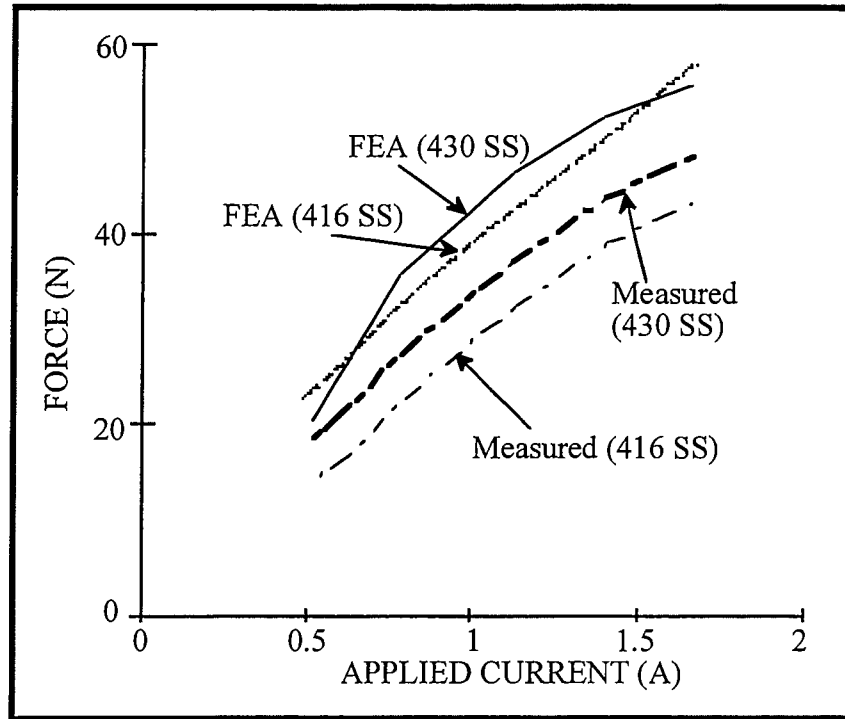


**Figure 10. Magnetic Force Comparison**

The accuracy of the FEA models was also verified by comparing FEA model inductance values with experimentally measured inductance values. The inductance calculation results were in reasonable agreement with experimental measurements (see table 2). The inductance values for open and closed air-gap cases were measured from four prototype solenoids using a recently calibrated digital inductance, capacitance, and resistance (LCR) meter (Hewlett Packard, 4263A) with an accuracy of  $\pm 0.05$  percent of the reading, and then the inductance values were averaged. The measurements were made at the lowest available frequency (100 Hz) to reduce eddy-current effects. The calculated values were obtained from the total magnetic co-energy value using the applied dc current to the FEA model. Figure 11 shows the flux density/magnetization force (B/H) curves used in the nonlinear FEA models in this study.

**Table 2. Inductance Value Comparison**

	Air Gap Opened	Air Gap Closed
Measured (@100 Hz)	597.2 mH	833.2 mH
FEA Result	588.0 mH	864.4 mH
Lumped Model Result	600 ±10 mH	

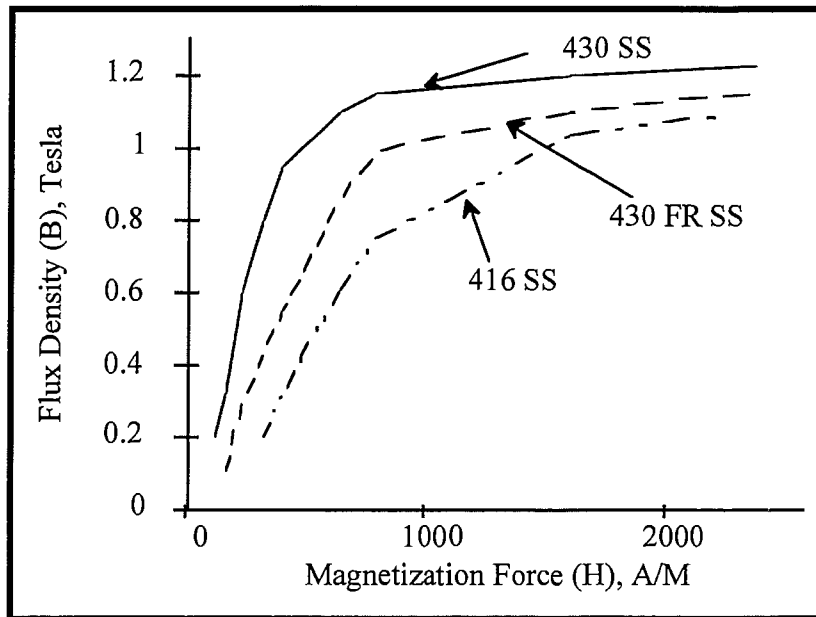


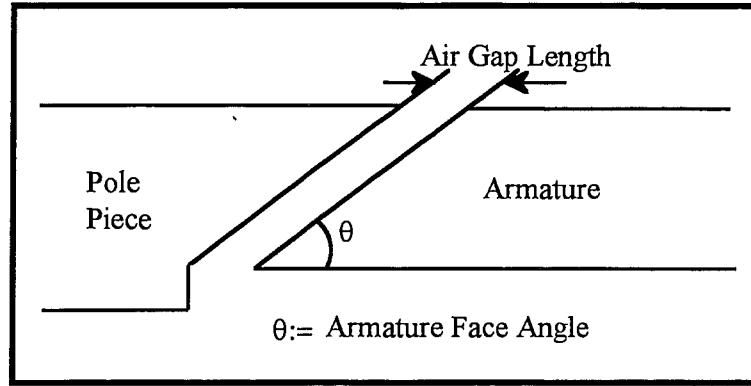
**Figure 11. B/H Curve for Plunger Magnetic Materials**

### FEA Force Calculation Results

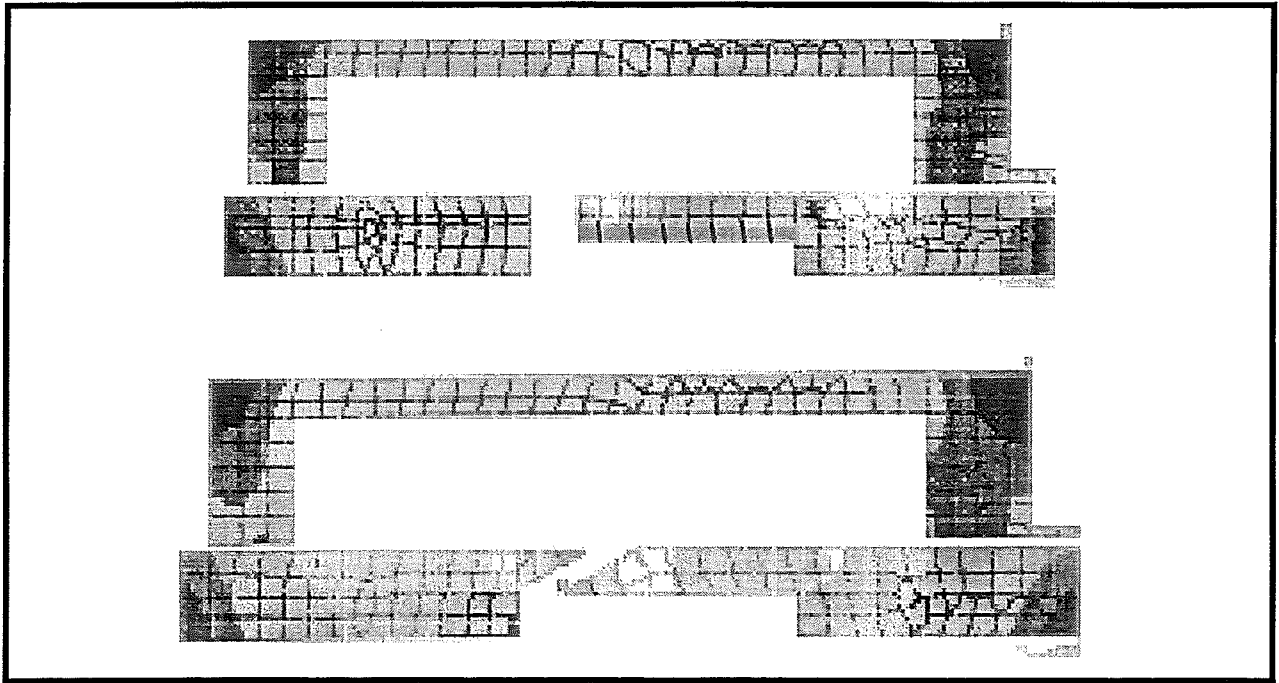
This section presents the FEA magnetic force calculations results. Specifically, the effects of armature face angle versus electromagnetic force, the electromagnetic force as a function of air-gap length, and the effect of the total number of coil turns are analyzed.

The mating faces of the pole piece and armature in the FSSV are cone shaped. The face angle of the design of record armature is  $30^\circ$  (see figure 12).

Two FEA models, one with a  $90^\circ$  and one with a  $30^\circ$  face angle, are shown in figure 13. The electromagnetic force was calculated using two different force calculation methods, virtual work method (co-energy method) and Maxwell's stress-tensor method. The accuracy of these two methods shows very close correlation. The effect of armature face angle on the magnetic force was calculated, and the results are shown in figure 14. The results reveal that  $30^\circ$  is the optimum armature face angle for maximizing electromagnetic force.



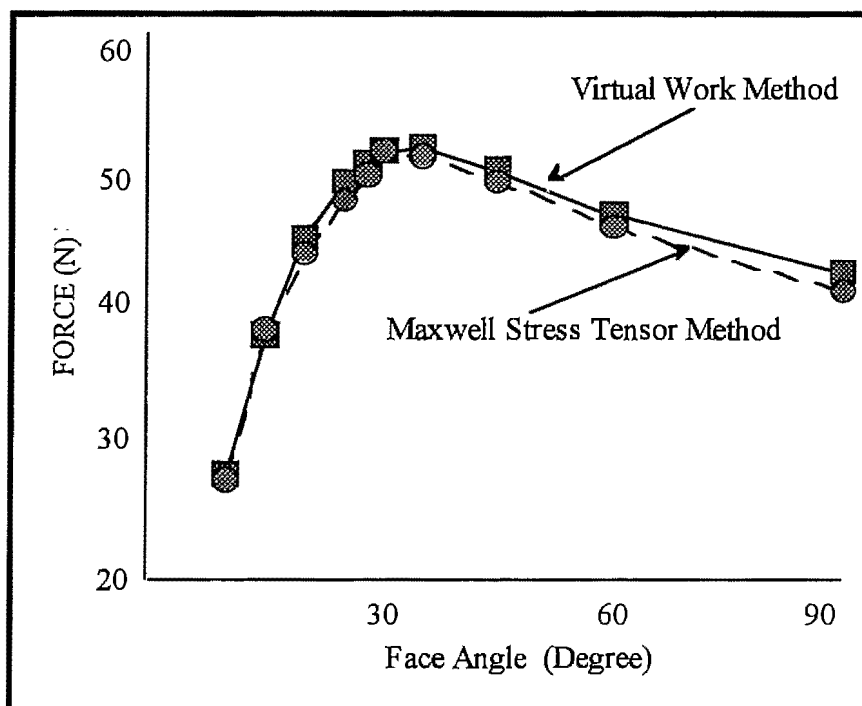
*Figure 12. Air Gap and Armature Face Angle*



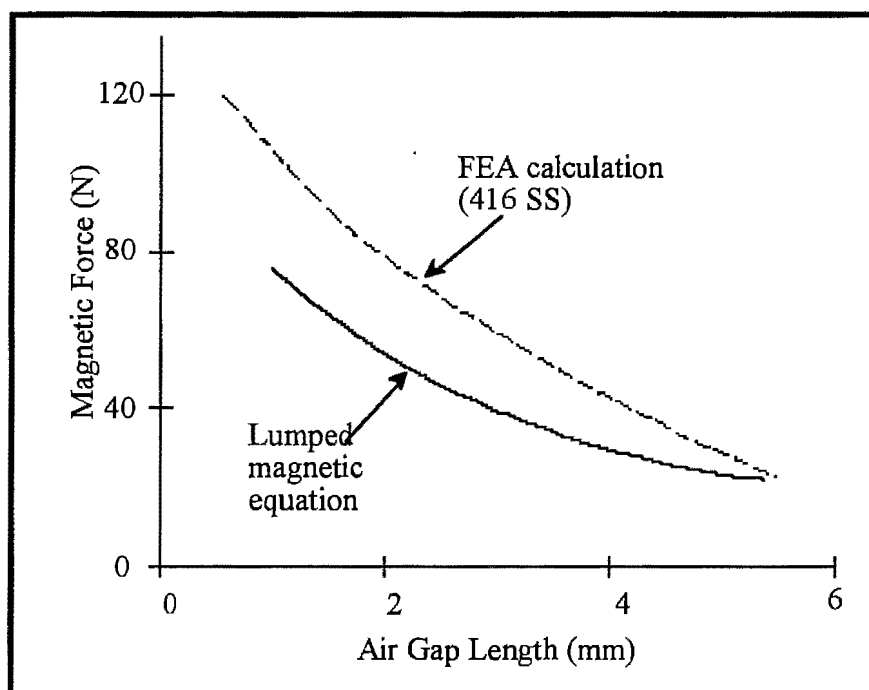
*Figure 13. FEA Models (Face Angle of  $90^\circ$  and  $30^\circ$ )*

Figure 15 depicts the magnetic force versus armature position (air-gap length between armature and pole piece). The FEA results are compared with the lumped magnetic circuit

results in a later section. The change in the magnetic force as a function of air gap is an important parameter to determine for future design considerations. In the present design, the magnitude of the air gap is fixed because that amount of armature travel distance is required to unseat the bore seal. However, future designs could incorporate a different sealing system, which might require less armature travel.



**Figure 14. Armature Face Angle vs Output Force (430SS)**



**Figure 15. Magnetic Force vs Air-Gap Length**



Figure 16 compares the total number of coil turns versus total output magnetic force. In this analysis, a constant current (1.25 A) is applied. The applied voltage is constant from the power source (30 Vdc). The same (dc) current at an increased number of turns may be obtained by using rectangular wire with an increased cross-sectional area to keep the total coil resistance constant. By increasing the number of coil turns from 2400 to 2800, the magnetic force in the closed position is increased up to 15-20 percent. In the actual torpedo, the valve is powered by a constant voltage source. Therefore, the effect of the number of coil turns on the magnetic force at a constant voltage was examined. The tradeoff to increase the number of turns is an increase in coil resistance and ultimately a decrease in coil amperage.

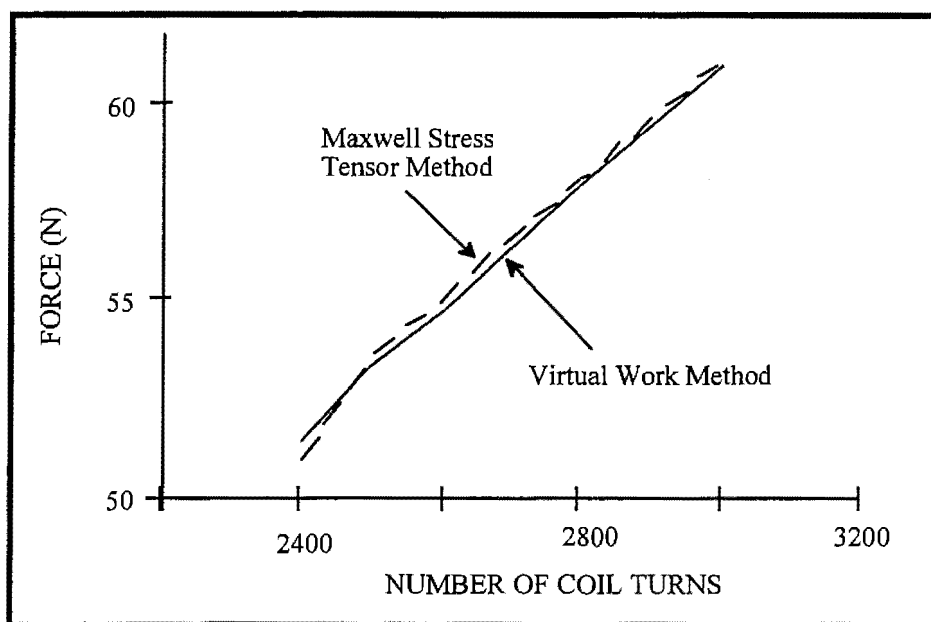


*Figure 16. Magnetic Force vs Total Number of Coil Turns (430 SS)*

## LUMPED MAGNETIC CIRCUIT ANALYSIS

This section presents the lumped parameter magnetic equations used for the solenoid magnetic force calculations and tradeoff studies. The lumped parameter magnetic equations are based on linear magnetic material properties and assume no saturation in the magnetic materials. Reluctance associated with the flux paths is not a function of the armature position. To formulate a lumped parameter magnetic equation, the magnetic flux paths from an FEA solution of a solenoid model were examined. The FEA result showed that the primary flux paths exist mainly in the magnetic material and that leakage occurs in the air-gap area, which is attributed to the fringing effect near the armature tips (see figure 3). Figure 17 shows the current and armature displacement of the valve versus time for a step input of voltage. The large dip in the current that occurs when the armature accelerates requires some explanation. It might seem at first consideration, that for a step change of voltage, the current should rise at a rate determined by the inductance to a level set by coil resistance only. As the armature begins to move inward,

the force on the armature would be that of the static (dc) force curve for that current. In fact, however, if a dc solenoid is connected to a power supply set at constant voltage, and the armature is allowed to close quickly, with a current-sensor or small resistor in the line and an oscilloscope (the changes are too fast to be seen on a D'Arsonval-type meter), it is observed that the current dips while the armature is moving. Conversely, if the power supply is set for constant current, the voltage rises during armature movement. A ballistic calculation of valve opening time that ignores this effect would lead to the conclusion that the valve would open faster than it actually would.

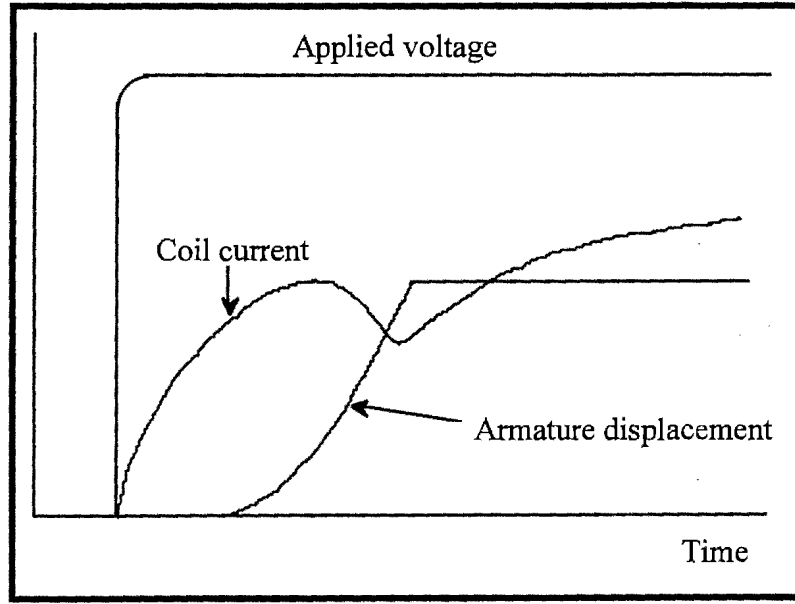


**Figure 17. Armature Displacement and Current vs Time for Step Voltage Input**

The power supplied by the source at constant voltage  $E_0$  is

$$P_s = E_0 i . \quad (1)$$

This power must equal that of dissipation in the resistive load, energy storage in the inductance  $L$ , and energy transfer to the external load:

$$P_{res} = i^2 r , \quad (2)$$

$$P_L = L(x) i \frac{di}{dt} , \quad (3)$$

$$P_{ext} = \frac{d}{dt} \left( \int F(x, i) dx \right) . \quad (4)$$

The above derivative with time is

$$P_{ext} = F(x, i) \frac{dx}{dt} + \int_a^x \frac{\partial F(s, i)}{\partial i} \left( \frac{di}{dt} \right) ds, \quad (5)$$

where  $a$  is a fixed constant, but the upper bound of integration is variable.

$$L = N^2 P, \quad (6)$$

$$E_0 i = i^2 r + N^2 P i \left( \frac{di}{dt} \right) + F(x, i) \frac{dx}{dt} + \int_a^x \frac{\partial F(s, i)}{\partial i} \left( \frac{di}{dt} \right) ds. \quad (7)$$

As the armature accelerates inward, the third term increases proportionally to speed. The partial derivative of the last term must also be positive (the force increases with current), and the left-side term is fixed. The equation can only be satisfied if  $di/dt$  is negative. The effect is somewhat comparable to back emf, well known to motor designers, but with additional complications.

The lumped parameter magnetic equation for magnetic force calculation derived from Roters (reference 2, article 72, equation 12a) is

$$F = k_1 k_2 \mu (ni)^2 \left[ \left( \frac{r_1}{x \cos \alpha} \right)^2 + \frac{1}{2} \sin^2 \alpha \right], \quad (8)$$

where

- $F$  = electromagnetic force on the plunger,
- $k_1$  = a constant related to geometry and units,
- $k_2$  = a dimensionless constant representing the fraction (squared) of total magnetomotive force present across the gap,
- $m$  = magnetic permeability of the fluid in the gap (assumed to be equal to that of free space),
- $n$  = number of turns on the coil,
- $i$  = electrical current in the coil,  $A$ ,
- $r$  = radius of an equivalent full cone,
- $x$  = plunger displacement ( $x = 0$  when plunger is pulled by electromagnetic force fully into the coil), and
- $\alpha$  = face angle of the plunger cone end, measured from a plane normal to the axis.

The above formula was derived by Roters from the more general relationship

$$F = k_1 k_2 \mu (ni)^2 \frac{dp}{dx}, \quad (9)$$

where  $p$  is magnetic circuit permeance, and the other symbols are as given above. The magnetic force versus plunger position result is plotted in figure 10.

## TEST RESULTS

Experimental tests were performed at the Naval Systems Division at Westinghouse to measure the differences in induced electromagnetic forces between a valve constructed of 416 SS and another made of 430 SS. A Tinius-Olson tensile machine was used to record the force at armature breakaway to the open position. The tensile breakaway force and displacement were recorded as a function of the voltage applied. Both valves had their springs removed so the magnetic forces could be better evaluated. This condition has been directly applied to FEA models and lumped magnetic circuit equations. Actual measurements showed that a valve constructed of 430 SS material has a magnetic force that is 15 to 25 percent greater than that of a valve constructed of 416 SS. The magnetic force measurement was also conducted at NUWC Composite Material Laboratory using an Instron Corporation Series IX Automated Material Testing System.

## MATERIAL SELECTION

This section presents information on the magnetic materials available for the solenoid and their selection criteria. In the early stages of the design process (prior to the electromagnetic design or preliminary design), a survey of materials can be conducted using general material properties. Many tradeoffs exist among the different magnetically soft magnetic materials, and it is necessary to define material selection criteria in the early stages of design and prototyping (references 7 and 8). A specific priority list of factors and their relative importance to one another must be constructed.

### Magnetic Core Materials

A solenoid consists of an armature, pole piece, and solenoid housing that should be selected for maximum magnetic flux-density handling capability and minimum eddy and hysteresis power losses. Additionally, low magnetic remanence (the tendency for a material to quickly lose magnetic field strength after the exciting coercive force (caused by current) has been removed, with very little magnetic field remaining) is also important. There are many solenoid soft magnetic materials available that offer various combinations of reduced losses, higher flux density saturation level, and lower cost. The solenoid soft magnetic material selection process is a tradeoff between efficiency, size, weight, complexity of manufacture, and cost of the solenoid to be designed.

In general, to be useful for magnetic poles, a material should have a high-magnetic saturation flux density and high permeability ( $B/H$ ) over much of its range. The magnetic hysteresis loop should be narrow (to avoid hysteresis losses and heating). The remanence ( $B_r$ ) should be small to prevent "sticking" on current valve shutoff. Electrical resistance should be high to help suppress

eddy currents. In addition, depending on the use of the valve, resistance to corrosion, mechanical strength, or surface-abrasion resistance may be useful.

Three general classes of stainless steel exist: austenitic, martensitic, and ferritic. The austenitic stainless steels (200- and 300- series), such as 302, 304, 316, 347 are not normally attracted to a magnet, although they may be faintly attracted if they have been severely cold-worked. They contain a significant amount of nickel (3.5 percent or more, and often 8 percent to 19 percent ), as well as chrome and iron, are more corrosion-resistant than other types, and can not be hardened by heat treatment. The martensitic and ferritic stainless steels (type 400 and 500), on the other hand, contain chrome and iron but little or no nickel, have generally less resistance to corrosion than austenitic stainless, and are magnetically permeable. Martensitic stainless steels can be hardened by heat treatment (410, 416, 440C, etc.), whereas the ferritic stainless steels (such as 430, etc.) can not. All the stainless steels contain some small amount of carbon (up to 1.2 percent ).

Although the 400-series stainless steels offer corrosion resistance, their magnetic properties are less useful than those of some other materials. If the valve parts could be surface-coated with some other material, performance could possibly be improved. The core material, for example, could be vanadium-permendur, silicon-iron, or iron with a very low carbon content; and these core materials could be coated by plating, for example, with nickel, titanium, or gold. A nickel coat could be made to be magnetically permeable as well as chemically inert. Core materials could be coated with aluminum, which could then be hard-anodized, followed by a fluorocarbon overcoat. The parts could be covered by an injection-molded layer of PPS or other plastic, and then perhaps machined back to a thin layer if necessary. It might also be possible to produce parts with a core of one material and a surface layer of another by powdered-metal technology, perhaps including subsequent hot isostatic pressing (HIP) and machining back, or surface-impregnating to reduce porosity.

In the history of the FSSV valve, the magnetically permeable components have been either 416 SS or 430 FR SS. Based on tests of parts made of particular batches of steel, 430 FR SS performed better at lower coercivities, while 416 SS has produced higher force at high current. However, the tests of particular parts of 416 cannot be entirely relied on because the magnetic properties of 416 SS are not controlled and may vary widely from batch to batch. The magnetic properties of 430 FR SS, on the other hand, are held within narrow limits because this alloy is produced specifically for use in magnetic circuits. The carbon content of 416 SS, for example, is specified as "not to exceed 0.15 percent," and could be anything from 0 to 0.15 percent. Carbon generally has a considerable effect on the magnetic properties of steel. The carbon content of 430 FR SS is held very near 0.06 percent. The silicon content of 416 SS is specified as "not to exceed 1.00 percent" and, again, may be much less; whereas, the silicon content of 430 FR SS is held near 1.25 percent. The addition of silicon generally improves the magnetic characteristics of steel. Thus, the published B/H curves of 416 SS may not always represent its actual performance; whereas, the curve for 430 FR SS should be reliable.

## Current-Carrying Wires

The common electric-conducting materials used in current-carrying wires for motors and electric machines are copper, aluminum, and copper-clad aluminum conductors. The most widely used conductor is solid copper wire because it is easy to wind and is readily soldered onto lead wires or terminal pins.

Aluminum wire tends to be brittle and difficult to work with. It is also difficult to terminate aluminum wire because it does not solder well. Moreover, solder joints with aluminum wire are subject to corrosion and are unreliable. Cladding aluminum wire with a thin layer of copper can reduce the termination difficulties, but the mechanical brittleness of the wire creates manufacturing problems. The thermal expansion of aluminum is higher than that of copper. Aluminum has about twice the electrical resistance of copper, but weighs about a third as much. Aluminum, therefore, is used where reduced weight is more important than higher volume for a given resistance or when cost is critical.

Figure 18 shows a variety of current-carrying wire types, and figure 19 depicts different multistranded wires. A hollow, conductor copper wire can be used for some very high-temperature electric machine, solenoid, and relay applications so that a cooling fluid can be pumped through the center. Multistranded wire is useful for high-frequency applications.

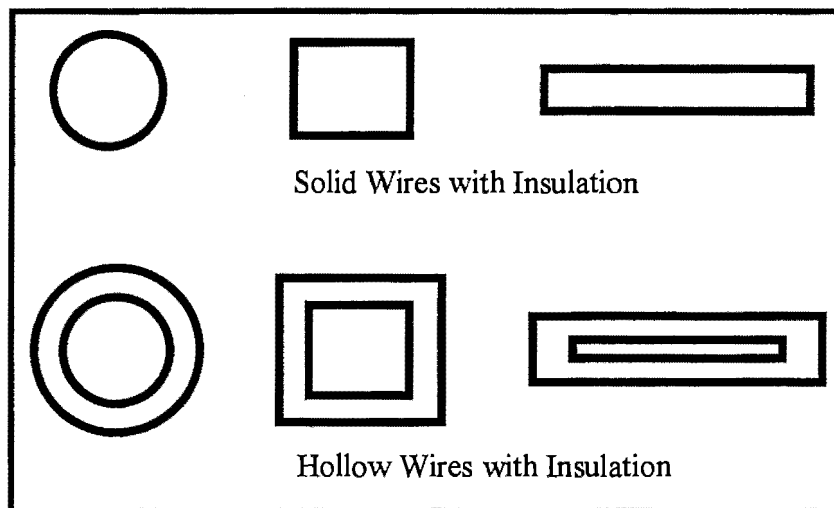


*Figure 18. Different Wire Types*

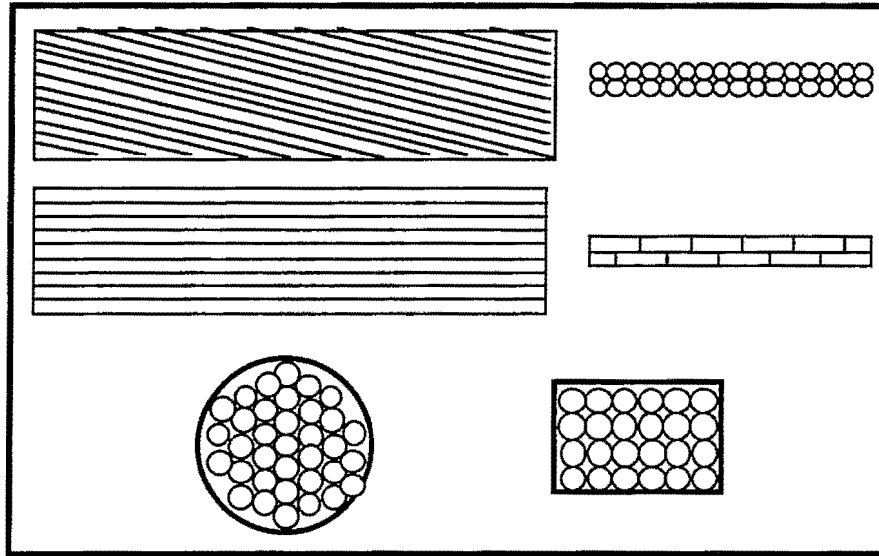


**Figure 19. Multistranded Wire Types**

Round cross-sectional electric conductor wire is the most common wire shape because it is easy to manufacture, insulate, and wind. Square or rectangular wire is used (1) in high-power density electromagnetic machine design when maximum use of the slot or winding area is mandatory and (2) in layer-wound coils, such as those in voice coil actuators and wound inductors, in which the maximum conductor packing factor is required. In a fixed volume, compared to round wire, rectangular wire offers as much as a 25-percent reduction in resistance because of the increased (up to 95 percent) packing factor of the conductor within the winding volume. Heat transfer from the coil is also enhanced by using rectangular wire with high-packing factor.

In a limited energy source, high-performance, high-power density electromagnetic device design, the reduction of conduction current ( $I^2R$ ) loss is a critical design issue. Therefore, a low-resistivity conductor should be used for minimum resistance to current flow, which minimizes  $I^2R$  loss. The rectangular solid conductor wire has a maximum cross-sectional area, so it has less resistance and results in less conduction current loss compared with the loss with round solid wire in a low-frequency application. As the frequency increases, the ac resistance of the rectangular-shaped wire increases at a faster increment than that of the round-shaped wire.

Current-carrying wires must be electrically insulated to prevent turn-to-turn shorts in a coil winding. A variety of polymeric insulation types with thermal ratings from 105°C (e.g., polyurethane) to 220°C (e.g., polyimide) are available. Factors affecting the choice of wire insulation include operating temperature, exposure of the winding to chemicals, wire bonding and soldering techniques, and cost (references 7 and 8).

## CONCLUSIONS

This memorandum describes the configuration of the fuel shutoff solenoid valve, which has a coil winding mounted inside the housing and pole piece and movable armature (plunger) in the middle of solenoid (figures 1 and 2). Two methods for modeling the solenoid, including 2-D FEA modeling and lumped magnetic circuit modeling, are also mentioned. In this memorandum, a 2-D axi-symmetry FEA model was used with enough flexibility to examine the influence of several design alternatives and manufacturability issues (armature face angle, air-gap length, and magnetic materials). Two well-known magnetic force calculation methods (virtual work method and Maxwell's stress tensor method) using FEA were compared, and it was found that the Maxwell's stress-tensor method requires more care to obtain accurate results than does the virtual work method.

As part of the overall performance assurance and optimization process, the electromagnetic force and tradeoff studies were analyzed using FEA and lumped magnetic circuit analysis. In particular, the influences of armature face angle, air-gap length, and magnetic material of the solenoid magnetic circuit with respect to the output force were examined (see figure 3). This memorandum reports some of the interesting conclusions of that study.

The general results of this study are summarized in table 3. It was found that the armature face angle has its own optimum, which is  $30^\circ$  from the axis. The magnetic properties of 430 SS FR are both better and much more uniform than those of 416 SS, thus improving reliability. Furthermore, using rectangular wire improves heat transfer from the coil because of the greatly reduced volume between wires. Accordingly, coil strength and reliability improves.

A 50-percent potential improvement in the opening force is possible if the recommended material and design changes are used.



**Table 3. Summary of Tradeoff Results**

<b>Design Changes</b>	<b>Magnetic Force Increase (%)</b>	<b>Tradeoffs</b>
<b>Magnetic Material (416 vs 430)</b>	10-15 %	Cost, fabrication difficulties
<b>Wire Shape /turns (2400 round vs 2800 rectangular)</b>	15-36%	Resistance held constant, 36% inductance increase, winding technique, cost
<b>Air Gap Length (5.5 mm vs 4.5 mm)</b>	10-12 %	Reduced valve open area, higher pressure drop

In this study, the 2-D FEA models were developed based on the convergence test results. Lumped magnetic circuit equations were also developed. The magnetic force and inductance calculations obtained from the FEA models and lumped magnetic models were compared with experimentally measured values from the prototype solenoids. Comparison of the calculations showed a close correlation.

In summary, this memorandum presents FEA modeling and analysis results that were performed during the performance assurance and optimization process for a fuel shutoff solenoid valve. The analysis shows interesting effects on magnetic forces by different design options: armature face angle, magnetic materials, number of coil turns, air-gap length, and applied current. Further, because of the interdependence of the magnetic fields in the solenoid and the current flowing in its coils under transient conditions, it is essential to combine the magnetic and electric circuit analysis. The simultaneous computation of fields and currents in, generally, nonlinear magnetic and electric circuits adds another measure of complexity to this complex research area.

## REFERENCES

1. G. P. Gogue and J. J. Stupak, *Electromagnetics Design Principles for Motors/Actuators*, PCIM, Universal City, CA, September 1991.
2. H. C. Roters, *Electromagnetics Devices*, John Wiley & Sons, NY, 1941.
3. C. P. Cho and B. K. Fussell, "Analysis of a Large-Horsepower Disc Rotor Axial Field, Brushless, Permanent Magnet Motor Using Finite Element and Lumped Parameter Circuit Analysis," *Proceedings of Incremental Motion Control Systems and Devices*, June 1992.
4. C. P. Cho and B. K. Fussell, "Analysis of a Large-Horsepower Axial Field, Brushless, PM Motor and the Effect of Rotor Misalignment," *Proceedings of Incremental Motion Control Systems and Devices Proceedings*, June 1993.
5. G. J. DeSalvo and R. W. Gorman, *ANSYS Engineering Analysis System User's Manual*, Swanson Analysis Systems, vols. 1 and 2, 1993.
6. M. C. Yaksh, "Electromagnetic Analysis of a Machine," *Proceedings of ANSYS User's Conference*, 1992.
7. A. Morcos, "A Primer on Magnetic Circuit Design: Materials, Permeance Calculations, and Finite Element Analysis," *MOTION*, January/February 1993, pp. 3-14.
8. M. Rippy, "An Overview Guide for the Selection of Lamination Materials," *MOTION*, September/October 1992, pp. 10-13.

## DISTRIBUTION

**External**

Naval Surface Warfare Center, Carderock Division, Annapolis Detachment  
(Code 80M -- J. Joynes)

**Internal**

Codes:	01	814
	10	82
	102	821
	104	822
	104 (Keshura)	8222
	20	8224
	22	8225
	38	823
	382	8231 (Barnett, Cho (5), Egan, Raposa,
	383	Thivierge)
	51122 (Routing copy)	8232 (Lisiewicz, Linskey, Michel)
	5131 (Conforti)	8233
	5141 (NPT Library (2))	8291 (Benson, Cancilliere, Hillenbrand)
	5142 (NLON Library)	8292
	60	83
	80	832
	81	833

**Total:     47**